Cortico-muscular synchronization by proprioceptive afferents from the tongue muscles during isometric tongue protrusion

Hitoshi Maezawa[a, *], Tatsuya Mima[b, c], Shogo Yazawa[d], Masao Matsuhashi[b], Hideaki Shiraishi[e], Makoto Funahashi[a]

[a] *Department of Oral Physiology, Graduate School of Dental Medicine, Hokkaido University, Kita-ku, Sapporo 060-8586, Japan*
[b] *Human Brain Research Center, Graduate School of Medicine, Kyoto University, Sakyo-ku, Kyoto 606-8507, Japan*
[c] *Graduate School of Core Ethics and Frontier Sciences, Ritsumeikan University, Kita-ku, Kyoto 603-8577, Japan*
[d] *Department of Systems Neuroscience, School of Medicine, Sapporo Medical University, Chuo-ku, Sapporo 060-8556, Japan*
[e] *Department of Pediatrics, Graduate School of Medicine, Hokkaido University, Kita-ku, Sapporo 060-8638, Japan*

Tables: 2
Figures: 5

*Corresponding author:
Hitoshi Maezawa, DDS, PhD
Department of Oral Physiology, Graduate School of Dental Medicine,
Hokkaido University, Kita-ku Kita 13 Nishi 7, Sapporo, Hokkaido 060-8586, Japan
TEL: 81-11-706-4229; FAX: 81-11-706-4229
E-mail: maezawa@den.hokudai.ac.jp

Abstract

Tongue movements contribute to oral functions including swallowing, vocalizing, and breathing. Fine tongue movements are regulated through efferent and afferent connections between the cortex and tongue. It has been demonstrated that cortico-muscular coherence (CMC) is reflected at two frequency bands during isometric tongue protrusions: the beta (β) band at 15–35 Hz and the low-frequency band at 2–10 Hz. The CMC at the β band (β-CMC) reflects motor commands from the primary motor cortex (M1) to the tongue muscles through hypoglossal motoneuron pools. However, the generator mechanism of the CMC at the low-frequency band (low-CMC) remains unknown. Here, we evaluated the mechanism of low-CMC during isometric tongue protrusion using magnetoencephalography (MEG). Somatosensory evoked fields (SEFs) were also recorded following electrical tongue stimulation. Significant low-CMC and β-CMC were observed over both hemispheres for each side of the tongue. Time-domain analysis showed that the MEG signal followed the electromyography signal for low-CMC, which was contrary to the finding that the MEG signal preceded the electromyography signal for β-CMC. The mean conduction time from the tongue to the cortex was not significantly different between the low-CMC (mean, 80.9 ms) and SEFs (mean, 71.1 ms). The cortical sources of low-CMC were located significantly posterior (mean, 10.1 mm) to the sources of β-CMC in M1, but were in the same area as tongue SEFs in the primary somatosensory cortex (S1). These results reveal that the low-CMC may be driven by proprioceptive afferents from the tongue muscles to S1, and that the oscillatory interaction was derived from each side of the tongue to both hemispheres. Oscillatory proprioceptive feedback from the tongue muscles may aid in the coordination of sophisticated tongue movements in humans.

Keywords: magnetoencephalography, cortico-muscular coherence, neural oscillation, muscle spindle, trigeminal nucleus, hypoglossal motor nucleus

1. Introduction

Sophisticated tongue movements play essential roles in vital oral functions such as speech articulation, mastication, swallowing, and airway patency. These fine tongue movements are accurately regulated by descending motor commands from the cortex to the tongue muscles and by afferent sensory feedback from the tongue muscles to the cortex. Such bi-directional functional connections between the cortex and muscles are mainly reflected in the cortico-muscular coherence (CMC) (Mima and Hallett, 1999; van Wijk et al., 2012).

The physiological interpretation of CMC varies according to the frequency band. The CMC in the beta (β) frequency band at 15–35 Hz (β-CMC) is generally thought to reflect the cortical interaction of motoneuron pools (Farmer et al., 1993; Mills and Schubert, 1995). Magnetoencephalography (MEG) and electroencephalography (EEG) studies have shown that the β-CMC is derived from the primary motor cortex (M1) and drives the muscle activities of the limbs and fingers through spinal motoneurons (MEG: Conway et al., 1995; Salenius et al., 1996, 1997; Brown et al., 1998; Gross et al., 2000) (EEG: Halliday et al., 1998; Mima et al., 2000). In our previous MEG study (Maezawa et al., 2014c), in addition to finding that the β-CMC for the thumb occurred over the contralateral hemisphere, we also found that the CMC for the tongue was detected at two different frequency bands (the β band and a low-frequency band at 2–10 Hz) over both hemispheres during isometric tongue protrusion for each side of the tongue. We concluded that the β-CMC for the tongue reflects the descending motor commands from M1 bilaterally to each side of the tongue through hypoglossal motoneuron pools. However, the mechanism of the CMC at the low-frequency band (low-CMC) is still unclear.

Recent studies on cortico-kinematic coherence (CKC) using an accelerometer demonstrated that the primary sensorimotor cortex (SM1) is strongly coherent at the low frequency band during repetitive finger movements (Piitulainen et al., 2013a, 2013b; Bourguignon et al., 2015). These studies suggest that the CKC at the low frequency band mainly reflects proprioceptive afferent input from muscle spindles to the contralateral SM1. Thus, as the human tongue muscles are rich in muscle spindles, the low-CMC for the tongue may be related to proprioceptive afferents from the tongue muscles.

The object of the present study was to investigate the generator mechanism of the low-CMC during human tongue protrusion using MEG. To do this, we first identified the conduction time of the low-CMC between the cortex and tongue, and compared it with the conduction times of the β-CMC and the somatosensory evoked fields (SEFs) following tongue stimulation. Second, we examined the location of the cortical sources for the low-CMC compared with the source locations of the β-CMC and tongue SEFs.

2. Materials and Methods

2.1. Subjects

Twenty-one right-handed healthy volunteers (14 men, 7 women; aged 20–37 years; mean age, 28.0 years) were studied. None of the subjects had a history of neurological or psychiatric disorders. Written informed consent was obtained from all subjects before they were included in the study. The protocol for this study was approved by the Ethical Committee of Dental Medicine of Hokkaido University. A portion of this study (β-CMC) has been reported previously using different analysis methods in 15 subjects (Maezawa et al., 2014c).

2.2. MEG recordings

Neuromagnetic signals were measured with a helmet-shaped 306-channel apparatus (VectorView, Elekta Neuromag, Helsinki, Finland) in a magnetically shielded room. This device had 102 trios that were composed of a magnetometer and a pair of planar gradiometers oriented orthogonally. Only 204 planar gradiometers were used for the analysis, detecting the largest signal above the corresponding generator source (Hämäläinen et al., 1993).

The exact position of the head with respect to the sensor array was determined by measuring the magnetic signals from four indicator coils placed on the scalp. The coil locations, as well as three predetermined landmarks on the skull, were identified with a three-dimensional digitizer (Isotrak 3S1002; Polhemus Navigation Sciences, Colchester, VT). This information was used to co-register the MEG signal and the individual magnetic resonance images (MRIs) obtained with a Signa Echo-Speed 1.5-Tesla system (General Electric, Milwaukee, WI).

2.2.1. Coherence recordings

Subjects performed a task requiring weak and sustained forward tongue protrusions (20–30% of the maximal strength on a subjective scale). The tongue movements required subjects to have their mouths open slightly, however they were asked not to touch their tongue to their lips to prevent any sensory feedback from the mouth and lips. The tongue protrusion task was performed for approximately 10–15 min, with each 2-min recording period being separated by a 30-s rest period. Surface electromyography (EMG) activity was recorded from the dorsum of the tongue bilaterally using disposable

EMG electrode pairs (Vitrode V, Nihon Kohden, Tokyo, Japan). Simultaneous recording of MEG and EMG signals was performed with a bandpass filter of 0.1–300 Hz and digitized at 997 Hz.

2.2.2. SEF recordings

SEFs were recorded following electrical tongue stimulation in 16 subjects (10 men, 6 women; aged 20–37 years; mean age, 29.5 years). Stimulation was applied on the right side of the tongue using an electrical stimulator (SEN-3401, Nihon Kohden, Tokyo, Japan). We used a pair of pin electrodes (400-μm diameter) with an inter-electrode distance of 3 mm for stimulation because they can safely deliver a low-intensity stimulus to a small oral region (Maezawa et al., 2008, 2011, 2014b). Tongue stimulation was applied 1 cm from the edge of the tongue, 3–4 cm from the tongue tip (Maezawa et al., 2014a). We confirmed through self-reports that electrical stimulation occurred only at the stimulation site. The stimulus consisted of square, biphasic, constant-current electric pulses (0.5 ms for 1 phase) applied once every 1 s. The intensity at each stimulation site was set to 2.5 to 3 times the sensory threshold for that stimulation site in each subject. Stimulation was applied at least 240 times. The recording passband was 0.1–330 Hz and the sampling rate was 997 Hz. The analysis window for averaging was from 100 ms before to 500 ms after each trigger signal. The baseline was calculated from -50 to -5 ms before stimulation onset.

2.3. Data analysis

2.3.1. Coherence analysis

For each side of the tongue, the EMG signals were high-pass filtered at 1 Hz and rectified to extract the motor unit potential timing information (Rosenberg et al., 1989). To calculate the spectral coherence between the MEG and rectified EMG signals at the low frequency band within 2–10 Hz, we used Welch's method (Welch, 1967) of spectral density estimation with a Hanning window, frequency resolution of 0.5 Hz, and half-overlapping samples, with the maximum frequency set to 15 Hz. To calculate the CMC spectrum at the β band, we again used Welch's method (Welch, 1967) with a Hanning window, frequency resolution of 0.5 Hz, and half-overlapping samples.

CMC values (Coh*xy*) were calculated according to the following equation:

$$\mathrm{Coh}xy(\lambda) = |\mathrm{R}xy(\lambda)|^2 = \frac{|fxy(\lambda)|^2}{fxx(\lambda) \cdot fyy(\lambda)}$$

In this equation, $fxx(\lambda)$ and $fyy(\lambda)$ are values of the auto-spectra of the MEG and rectified EMG signals for a given frequency λ, and $fxy(\lambda)$ is the cross-spectrum between them. The muscular-muscular coherence (MMC) spectrum between sides of the tongue was also calculated in the same manner as the β-CMC spectrum.

We excluded the initial 5 s of each EMG signal recorded during the task from the analysis. We also rejected epochs with artifacts identified by visual inspection for either side from the analysis, thus yielding 620 ± 122 (mean ± standard deviation) total samples. Based on the method by Rosenberg et al. (1989), coherence above Z was considered to be significant at $p < 0.01$, where $Z = 1-0.01^{(1/L-1)}$. L was the total number of samples used in the estimation of the auto- and cross-spectra.

A cross-correlogram in the time domain was investigated by applying an inverse Fourier transformation to the averaged cross-spectrum of the right side of the tongue for each frequency band (low-frequency band and β band). Next, we constructed isocontour

maps at the time points that showed cross-correlogram peaks for each frequency band. Equivalent current dipoles (ECDs) were used to model the sources of the oscillatory MEG signals. A spherical head model was used to estimate the location of the ECDs over the contralateral (left) hemisphere for each frequency band. The center of this head model fit the local curvature of the surface of an individual's brain, as determined by their MRIs (Sarvas, 1987). Only ECDs attaining an 85% goodness-of-fit and a confidence volume smaller than 3000 mm^3 were accepted.

2.3.2. SEF analysis

The peak latency of SEFs was measured from the channel showing the maximal signal over the contralateral (left) hemisphere. Isocontour maps were constructed at the peak latency. The digitized shape of each subject's head was fitted using a simple spherical head model. The magnetic field sources were modeled as ECDs whose locations were estimated from the measured magnetic waveforms. Only ECDs attaining a 90% goodness-of-fit and a confidence volume smaller than 1000 mm^3 were accepted.

2.4. Statistics

Data are expressed as the mean ± the standard error of the mean (SEM). The coherence value was normalized with an arc hyperbolic tangent transformation to stabilize the variance (Halliday et al., 1995). The frequency and values of the low-CMC were compared using two-way repeated measures analyses of variance (ANOVAs) with the within-subjects factors of tongue side (right vs. left) and hemisphere (contralateral vs. ipsilateral). Post hoc comparisons were performed using paired *t*-tests with Bonferroni corrections after significant effects were found. The time lag of the

low-CMC and the peak latency of SEFs were analyzed using paired *t*-tests. The contralateral ECD locations in each axis (*x*-axis, *y*-axis, and *z*-axis) were analyzed for the CMCs at the two frequency bands (low-frequency band and β band) and for SEFs using repeated measures ANOVAs with Bonferroni corrections (low-CMC vs. β-CMC vs. SEFs). The *x*-axis passes through the preauricular points from left to right, the *y*-axis passes through the nasion, and the *z*-axis points upward from the plane determined by the *x*- and *y*-axes. The statistical significance level was set to $p < 0.05$. Significance levels were corrected for multiple comparisons.

3. Results

3.1. Coherence

Figure 1 shows examples of the EMG signals from both sides of the tongue during tongue protrusion in subject 10. We could detect cyclical EMG activity of the tongue at the low-frequency band, and such cyclical EMG activity was synchronized between sides of the tongue.

Figure 2 provides the power spectra of the MEG signal from the right sensorimotor cortex and of the EMG from the left side of the tongue in subject 10 during the tongue protrusion task. Distinct MEG peaks were detected at the low-frequency band (10 Hz) and β band (19 Hz) (Fig. 2A[1]). The EMG and MMC spectra between the sides of the tongue also showed peaks at the low-frequency bands (3 and 7 Hz) and β band (24 Hz) (Fig. 2A[2], 2B). Thus, the power spectra of the EMG and MMC signals had peaks at the same frequency bands.

Figure 2C shows the CMC spectra recorded from the left [1] and right [2] sides of the tongue in subject 10. Two distinct peak frequencies were identified in the

low-frequency band over both hemispheres for each side of the tongue. Coherent signals were also detected in the β band bilaterally for each tongue side.

3.1.1. MMC between tongue sides

Significant MMC between the sides of the tongue was detected at two frequency bands: 2–10 Hz and 15–30 Hz. The low-frequency band had two distinct peaks at 2–4 Hz (first peak) and 6–10 Hz (second peak) (Table 1).

3.1.2. CMC

3.1.2.1. Low-CMC

Table 1 shows the peak frequencies of the low-CMC across subjects. The low-CMC had two distinct peaks: 2–5 Hz (first peak) and 6–10 Hz (second peak). The means of the first and second peak frequencies for each side of the tongue over each hemisphere are also shown in Table 1. The ANOVA did not reveal a significant main effects for the frequency of coherence between tongue sides ($p = 0.854$ [first peak], $p = 0.889$ [second peak]) or hemispheres ($p = 0.439$ [first peak], $p = 0.077$ [second peak]).

The means of the CMC values of the first and second peak frequencies for each side of the tongue over each hemisphere are shown in Table 2. The shape and value of the waveforms were variable across subjects (Supplementary Figure). The ANOVA did not reveal a significant main effect for the magnitude of coherence between hemispheres ($p = 0.576$ [first peak], $p = 0.066$ [second peak]) or tongue sides ($p = 0.405$ [first peak], $p = 0.566$ [second peak]).

3.1.2.2. β-CMC

The mean frequency for each hemisphere was 25.8 ± 1.5 Hz (contralateral, N = 18) and 23.0 ± 1.4 Hz (ipsilateral, N = 14) for the right side, and 24.0 ± 1.3 Hz (contralateral, N = 18) and 22.9 ± 1.5 Hz (ipsilateral, N = 17) for the left side of the tongue.

The mean CMC values for each side of the tongue over each hemisphere are shown in Table 2.

3.2. Time estimation of the CMC and SEFs

Figure 3 shows the waveforms of the cross-correlogram and SEF over the contralateral hemisphere for the right side of the tongue in subject 10. The peak latency of the cross-correlogram for the low-CMC was observed after EMG onset (Fig. 3A[1]), while the peak latency of the β-CMC was detected before EMG onset (Fig. 3A[2]).

Figure 4 compares the mean conduction times between the tongue and cortex across the subjects who meet the criteria for the source localization analysis for CMC and SEFs (low-CMC [N = 15], β-CMC [N = 14], SEFs [N = 16]). No significant differences in peak latency were detected between the low-CMC and the SEFs ($p = 0.216$).

3.3. Source localization of the CMC and SEFs

The isofield contour maps revealed a dipolar pattern at the latency showing the maximum amplitude for the CMC and SEFs in a representative subject (subject 10) (Fig. 3B[1–3]). The ECDs of the low-CMC and SEFs were located in the lateral part of the central sulcus, which suggests they were in the tongue region of the primary somatosensory cortex (S1) (Fig. 3C). The ECDs of the β-CMC were located in the anterior part of the central sulcus, which suggests they were in the tongue region of M1.

The directions of the ECDs were similarly posterior for the low-CMC and the SEFs, but were anterior for the β-CMC (Fig. 3C).

The isofield contour maps showed a dipolar pattern at the latency showing the maximum amplitude for the CMC and SEFs in all subjects. Estimating the ECD locations, the cortical sources of the low-CMC and SEFs were located around the central sulcus, and the sources of the β-CMC were located in the inferior part of the central sulcus. The ANOVA revealed a significant main effect for the ECD locations in each axis ($p = 0.019$ [*x*-axis], $p < 0.001$ [*y*-axis], $p = 0.033$ [*z*-axis]). The statistical analysis indicated that the ECDs for the low-CMC were located significantly posterior (mean, 10.1 mm; $p < 0.001$) to those for the β-CMC, but not significantly inferior (mean, 5.4 mm; $p = 0.333$) or lateral (mean, 4.5 mm; $p = 0.127$) (Fig. 5). Moreover, the ECD locations for the low-CMC were not significantly different to those of the SEFs at each axis (posterior: mean, 2.2 mm, $p = 0.034$; superior: mean, 4.5 mm, $p = 0.025$; medial: mean, 3.1 mm, $p = 0.333$). The ECD locations for the SEFs were located significantly posterior (mean, 7.9 mm; $p = 0.006$), inferior (mean, 9.9 mm; $p = 0.012$), and lateral (mean, 7.6 mm; $p < 0.001$) to those for the β-CMC.

The ECD orientations of the low-CMC were posterior in 14 subjects and anterior in two subjects. The ECD directions of the β-CMC were variable among subjects, but those of the SEFs were posterior in all subjects.

4. Discussion

The present study demonstrates that the generator mechanism of the tongue CMC differed depending on the frequency band (low-frequency band vs. β band) during isometric tongue protrusion in humans. The low-CMC reflects functional coupling

related to proprioceptive feedback from the tongue muscles to the cortex, in contrast with the β-CMC, which reveals the efferent motor commands from the cortex to the tongue muscles.

4.1. Generator mechanism of the low-CMC

Sophisticated tongue movements can be regulated accurately through the bi-directional information flow between the cortex and tongue. The unidirectional functional coupling from the cortex to the tongue was reflected by the β-CMC through the hypoglossal motor nucleus, which innervates the tongue muscles, during tongue protrusion in humans (Maezawa et al., 2014c). On the other hand, despite the fact that the other direction of the afferent pathway plays a role in the genesis of forearm CMC (Riddle and Barker, 2005, 2006), little is known about the tongue CMC related to afferent sensory feedback.

Previous studies have reported that CMC was detected at low-frequency band (Wessberg and Vallbo, 1995; Gross et al., 2002) during repetitive slow finger movements. Recent CKC studies also detected the coupling between the cortex and finger at the low-frequency band of repetitive finger movements (Piitulainen et al., 2013a, 2013b; Bourguignon et al., 2015). These studies concluded that SM1 was primarily activated by proprioceptive reafferents. In the present study, given that the MEG signal for the low-CMC followed the EMG signal in time and that the cortical sources of the low-CMC originated from S1, this implies that the low-CMC reflects the proprioceptive afferents from the tongue to the cortex.

Three different types of peripheral sensory inputs related to proprioception exist: joint receptors, cutaneous receptors, and muscle spindles. Unlike most skeletal muscles,

the tongue, as a visceral muscle, does not have a joint, and therefore has no joint receptors. Thus, we can exclude the effect of joint afferents in the generation of the low-CMC. Moreover, the effect of cutaneous sensation was insignificant in the present study. Piitulainen et al. (2013a) reported that finger CKC is mainly due to the proprioception from finger muscle spindles during flexion-extension movements, with cutaneous inputs having a negligible effect. The authors suggested that this is because ‘‘gating’’ of cutaneous inputs occurred during finger movements, which was indicated by the fact that the intensities of cutaneous stimuli were perceived as being weaker (Milne et al., 1988), with higher perceptual thresholds (Angel and Malenka, 1982). Therefore, we can exclude the effects of joint and cutaneous receptors for the mechanism of low-CMC. In the present study, we could detect cyclical EMG activity of the tongue at low-frequency band during the tonic contraction, and such cyclical EMG activity was synchronized between sides of the tongue. As the EMG power spectra and MMC between the two sides of the tongue showed low-frequency peaks, we concluded that the low-CMC might reflect cyclical proprioceptive feedback from the muscle spindles of the tongue. Thus, we concluded that the low-CMC related to proprioception might serve as a sensorimotor feedback loop consisting of M1-muscle-S1-M1 network, and that such proprioceptive feedback may make it possible for M1 to regulate fine and flexible movement of the tongue during vital oral functions, such as mastication, swallowing, respiration and speech.

From among the mammalian species, the muscle spindles of the tongue have only been observed in primates (Cooper, 1953). The sensory feedback through the muscle spindles of the tongue may contribute to fine oral functions. In particular, as the muscle spindles of the tongue are highly developed in humans compared with those in other

primates, proprioception from the tongue muscle spindles in humans may play an important role in speech production. Ruspantini et al. (2012) reported that the low oscillatory frequency related to proprioceptive afferent feedback from the mouth muscles might play an important role in the smooth and sophisticated oral movements generated during word production. Moreover, the low-CMC related to proprioception may play critical role for keeping tongue position. It was sometimes difficult to keep steady tongue position due to the lack of attachment between intrinsic tongue muscles and bones. As we could detect cyclical EMG activity at low-frequency band, the monitoring system for tongue position through sensorimotor feedback loop may make it possible to maintain stable tongue posture as a whole. In fact, a study by Murayama et al. (2001) detected low-CMC at 7–11 Hz for paraspinal and abdominal muscles in the body trunk, suggesting that low-CMC might help axial muscles work together during postural control (Marsden et al., 1999). In addition, the presence of physiological tremor may underlie the low-CMC. A study by Jerbi et al. (2007) showed significant and slow oscillatory activity (2–5 Hz) over the contralateral S1 during a continuous hand visuomotor task, with time-varying hand speeds. Since tongue muscles are characteristically free-moving, it is possible that the subjects' tongues exhibited involuntary slight tremulous movements during the isometric tongue protrusion task. Future studies should measure the CKC during the isometric tongue protrusion task using an accelerometer.

4.2. Conduction time of the afferent pathways

To estimate the conduction time through afferent pathways from the periphery to the cortex related to cutaneous sensation, we generally use the somatosensory evoked

potentials (SEPs) or SEFs following stimulation of a target peripheral region (Mauguière et al., 1999; Burgess et al., 2011). A previous study investigating the CMC during finger movements estimated that the time lag from the finger to the cortex through the afferent pathway was obviously greater than the initial component (N20m) of SEPs following median nerve stimulation (Witham et al., 2011). The reason for the longer latency of the CMC time lag compared with that of the N20m of SEPs was that the CMC time lag might reflect the average of all SEP components, not just the initial component; additionally, the afferent pathway and nerve fiber sizes are different between cutaneous sensation and proprioceptive sensation. Below, we discuss the two reasons for why we believe the time lag of the low-CMC also reflected the "averaged" cortical response of all of the components related to proprioception from the tongue muscles.

First, the initial component of SEFs following electrical tongue stimulation occurs at 19 ms with an anterior current orientation (Sakamoto et al., 2008). However, since the initial component of tongue SEFs is sometimes hard to detect due to its small amplitude, the prominent components that occur at the middle latency with a posterior current orientation are often used as a reliable and stable parameter for tongue SEFs (Nakahara et al., 2004; Maezawa et al., 2008, 2011, 2014a). In the present study, as the mean time lag and current orientation of the low-CMC were consistent with those of middle-latency tongue SEF components, the low-CMC may reflect the cortical response of middle-latency components related to proprioception.

Second, a previous study on SEFs following passive finger movement reported four main components over the contralateral hemisphere: 1M(P) (mean, 19.4 ms), 2M(P) (46.0 ms), 3M(P) (70.0 ms), and 4M(P) (119.0 ms) (Xiang et al., 1997). Among these

components, 2M(P) and 3M(P) were the most notable and stable, but the initial component of 1M(P) at around 20 ms had a small amplitude and was detected in only three of the ten subjects. Another SEF study related to proprioception reported responses over the contralateral hemisphere at 78.7 ms (M70) following motor-point electrical stimulation applied to the right extensor indicis muscles using a pair of wire electrodes (Onishi et al., 2011). The authors concluded that the M70 component, whose onset latency occurred approximately 40 ms after the motor-point stimulation, must not reflect the initial cortical response of proprioceptive afferents, since the initial proprioceptive response at the thalamus level after motor-point stimulation of the extensor digitorum muscles was confirmed to occur at 10–12 ms by direct recording (Fukuda et al., 2000). Given the constant results showing detection of middle-latency SEF components related to proprioception from the finger, we conclude that the low-CMC may also reflect the prominent cortical response of middle-latency components, not the initial component, through afferent feedback from the tongue muscles.

4.3. Source location

In the present study, since the low-CMC sources were significantly different from M1 (generator of the β-CMC), but were consistent with S1 (generator of the SEFs), we concluded that low-CMC generation may mainly originate from S1.

Potential candidates for generating the low-CMC include all of the areas in S1 that receive proprioceptive afferents, such as areas 1, 2, 3a, and 3b. Several animal studies have shown that areas 3a and 2, and areas 3b and 1 process different sensory information that reaches S1: areas 3b and 1 receive mainly cutaneous tactile inputs

(Kaas, 1983), whereas areas 3a and 2 receive mainly proprioceptive inputs from joint and muscle receptors. In particular, it has been well established that most neurons in area 3a are associated with muscle afferents (Lucier et al., 1975; Jones and Porter, 1980), in contrast with area 2, which is best activated by joint movements (Burchfiel and Duffy, 1972; Schwarz et al., 1973; Mima et al., 1997). Since the tongue has muscle spindles, but not joint receptors, it is reasonable that the source of the low-CMC is located in area 3a of S1. However, since the MEG system is inherently biased toward detecting activation in the tangential cortex, and since the current orientation generated in area 3a is mainly radial, it was difficult to record the activation in area 3a using MEG. As the low-CMC was large in amplitude, the generators of the low-CMC should be located mainly by tangential generators. Since the current orientation generated in area 1 is mainly radial, area 1 was also excluded as the potential generator of the low-CMC. These results regarding the potential cortical generators in S1 suggest that area 3b is the main region responsible for the low-CMC.

Self-paced repetitive finger movements at 2 Hz were found to be associated with steady-state movement-related magnetic fields (ssMRMFs) in a study by Gerloff et al. (1998). They observed that ssMRMFs had two main components after EMG onset: a motor field component (MF) that peaked at 37 ms with an anterior current orientation, and a postmovement field component (post-MF) that peaked at 102 ms with a posterior current orientation. Of these two components, the post-MF component originating from S1 had an obviously larger amplitude than the MF component from M1. The authors concluded that the MF component was mainly related to a corticospinal volley from M1, whereas the post-MF component represented reafferent feedback processing from the muscle spindles to S1 (Gerloff et al., 1998). Regarding the similarity in the conduction

time of the afferent pathway and the current orientation between the post-MF and low-CMC, the low-CMC may reflect a component similar to the post-MF component in ssMRMFs. Given that, in monkeys, neurons in area 3b receive muscle afferents mainly via area 3a, it is reasonable that the activation of low-CMC in area 3b may spread from neurons in area 3a, receiving the initial proprioceptive response from tongue muscle spindles. Anatomically, proprioceptive fibers from the muscle spindles of the tongue run through the hypoglossal nerve and end in the trigeminal nuclei of the brainstem (Fitzgerald and Sachithanandan, 1979). Thus, such proprioceptive responses are directed through the trigeminal nuclei from the tongue muscle spindles to area 3a in S1.

4.4. Limitations

The direction of information flow between the cortex and muscles can also be inferred using partial directed coherence analysis (Schelter et al., 2005; Faes and Nollo, 2010). Mima et al. (2001) reported that the efferent CMC at the β-frequency band from the cortex to the muscles was larger than that in the opposite direction during finger muscle contraction. Recently, Bourguignon et al. (2015) concluded that CKC mainly reflects movement-induced proprioceptive feedback to SM1. Additional analysis is needed to explore the direction of information flow between the cortex and tongue muscles at the low-frequency band by means of partial directed coherence analysis.

4.5. Conclusions

In conclusion, our results show that the oscillatory synchronization at 2–10 Hz is due to proprioceptive afferent feedback from the muscle spindles of the tongue, and that the functional coupling at 2–10 Hz may be derived from each side of the tongue to the

bilateral S1. Such oscillatory proprioceptive feedback from the tongue may play an important role in fine-tuning oral movements when masticating, swallowing, and speaking. Moreover, in clinical situations, identifying the CMC in the oral region might help elucidate the central pathophysiological mechanisms underlying oral dystonia or dyskinesia.

Acknowledgements

This work was supported by Grants-in-Aid for Scientific Research (B)24300192 (TM), (C)23591488 (HS), and (C)25462883 (MF), and Grants-in-Aid for Young Scientists (B)25862071 (HM) from the Japan Society for the Promotion of Science.

References

Angel, R.W., Malenka, R.C., 1982. Velocity-dependent suppression of cutaneous sensitivity during movement. Exp. Neurol. 77, 266–274.

Bourguignon, M., Piitulainen, H., De Tiège, X., Jousmäki, V., Hari, R., 2015. Corticokinematic coherence mainly reflects movement-induced proprioceptive feedback Neuroimage 106, 382–390.

Brown, P., Salenius, S., Rothwell, J.C., Hari, R., 1998. Cortical correlation of the Piper rhythm in humans. J. Neurophysiol. 80, 2911–2917.

Burchfiel, J.L., Duffy, F.H., 1972. Muscle afferent input to single cells in primate somatosensory cortex. Brain Res. 45, 241–246.

Burgess, R.C., Funke, M.E., Bowyer, S.M., Lewine, J.D., Kirsch, H.E., Bagić, A.I.; ACMEGS Clinical Practice Guideline (CPG) Committee, 2011. American Clinical Magnetoencephalography Society Clinical Practice Guideline 2: presurgical functional brain mapping using magnetic evoked fields. J. Clin. Neurophysiol. 28, 355–361.

Conway, B., Halliday, D., Farmer, S.F., Shahani, U., Maas, P., Weir, A.I., Rosenberg, J.R., 1995. Synchronization between motor cortex and spinal motoneuronal pool during the performance of a maintained motor task in man. J. Physiol. 489, 917–924.

Cooper S., 1953. Muscle spindles in the intrinsic muscles of the human tongue.

J. Physiol. 122, 193–202.

Faes, L., Nollo, G., 2010. Extended causal modeling to assess Partial Directed Coherence in multiple time series with significant instantaneous interactions. Biol. Cybern. 103, 387–400.

Farmer, S.F., Bremner, F.D., Halliday, D.M., Rosenberg, J.R., Stephens, J.A., 1993. The frequency content of common synaptic inputs to motoneurons studied during voluntary isometric contraction in man. J. Physiol. 470, 127–155.

Fitzgerald, M.J., Sachithanandan, S.R., 1979. The structure and source of lingual proprioceptors in the monkey. J. Anat. 128, 523–552.

Fukuda, M., Kameyama, S., Tanaka, R., 2000. Thalamic potentials evoked by motor point stimulation. Muscle Nerve. 23, 246–251.

Gerloff, C., Uenishi, N., Nagamine, T., Kunieda, T., Hallett, M., Shibasaki, H., 1998. Cortical activation during fast repetitive finger movements in humans: steady-state movement-related magnetic fields and their cortical generators. Electroencephalogr. Clin. Neurophysiol. 109, 444–453.

Gross, J., Tass, P.A., Salenius, S., Hari, R., Freund, H., Schnitzler, A., 2000. Cortico-muscular synchronization during isometric muscle contraction in humans as revealed by magnetoencephalography. J. Physiol. 527, 623–631.

Gross, J., Timmermann, L., Kujala, J., Dirks, M., Schmitz, F., Salmelin, R., Schnitzler, A., 2002. The neural basis of intermittent motor control in humans. Proc. Natl. Acad. Sci. U. S. A. 99, 2299–2302.

Halliday, D.M., Rosenberg, J.R., Amjad, A.M., Breeze, P., Conway, B.A., Farmer, S.F., 1995. A framework for the analysis of mixed time series/point process data--theory and application to the study of physiological tremor, single unit discharges and electromyograms. Prog. Biophys. Mol. Biol. 64, 237–278.

Halliday, D.M., Conway, B.A., Farmer, S.F., Rosenberg, J.R., 1998. Using electroencephalography to study functional coupling between cortical activity and electromyograms during voluntary contractions in humans. Neurosci. Lett. 23, 5–8.

Hämäläinen, M., Hari, R., Ilmoniemi, R.J., Knuutila, J., Lounasmaa, O.V., 1993. Magnetoencephalography-theory, instrumentation, and applications to noninvasive studies of the working human brain. Rev. Mod. Phys. 65, 413–497.

Jerbi, K., Lachaux, J.P., N'Diaye, K., Pantazis, D., Leahy, R.M., Garnero, L., Baillet, S., 2007. Coherent neural representation of hand speed in humans revealed by MEG imaging. Proc. Natl. Acad. Sci. U S A. 104, 7676–7681.

Jones, E.G., Porter, R., 1980. What is area 3a? Brain Res. 203, 1–43.

Kaas, J.H., 1983. What, if anything, is SI? Organization of first somatosensory area of cortex. Physiol. Rev. 63, 206–231.

Lucier, G.E., Rüegg, D.C., Wiesendanger, M., 1975. Responses of neurones in motor cortex and in area 3A to controlled stretches of forelimb muscles in cebus monkeys. J. Physiol. 251, 833–853.

Maezawa, H., Yoshida, K., Nagamine, T., Matsubayashi, J., Enatsu, R., Bessho, K., Fukuyama, H., 2008. Somatosensory evoked magnetic fields following electric tongue stimulation using pin electrodes. Neurosci. Res. 62, 131–139.

Maezawa, H., Yoshida, K., Matsuhashi, M., Yokoyama, Y., Mima, T., Bessho, K., Fujita, S., Nagamine, T., Fukuyama, H., 2011. Evaluation of tongue sensory disturbance by somatosensory evoked magnetic fields following tongue stimulation. Neurosci. Res. 71, 244–250.

Maezawa, H., Hirai, Y., Shiraishi, H., Funahashi, M., 2014a. Somatosensory evoked magnetic fields following tongue and hard palate stimulation on the preferred chewing side. J. Neurol. Sci. 347, 288–294.

Maezawa, H., Matsuhashi, M., Yoshida, K., Mima, T., Nagamine, T., Fukuyama, H., 2014b. Evaluation of lip sensory disturbance using somatosensory evoked magnetic fields. Clin. Neurophysiol. 125, 363–369.

Maezawa, H., Mima, T., Yazawa, S., Matsuhashi, M., Shiraishi, H., Hirai, Y., Funahashi, M., 2014c. Contralateral dominance of corticomuscular coherence for both sides of the tongue during human tongue protrusion: an MEG study. Neuroimage 101, 245–255.

Marsden, J.F., Farmer, S.F., Halliday, D.M., Rosenberg, J.R., Brown, P., 1999. The unilateral and bilateral control of motor unit pairs in the first dorsal interosseus and paraspinal muscles in man. J. Physiol. 521, 553–564.

Mauguière, F., Allison, T., Babiloni, C., Buchner, H., Eisen, A.A., Goodin, D.S., Jones, S.J., Kakigi, R., Matsuoka, S., Nuwer, M., Rossini, P.M., Shibasaki, H., 1999. Somatosensory evoked potentials. The International Federation of Clinical Neurophysiology. Electroencephalogr. Clin. Neurophysiol. Suppl. 52, 79–90.

Mills, K.R., Schubert, M., 1995. Short time synchronization of human motor units and their responses to transcranial magnetic stimulation. J. Physiol. 483, 511–523.

Milne, R.J., Aniss, A.M., Kay, N.E., Gandevia, S.C., 1988. Reduction in perceived intensity of cutaneous stimuli during movement: a quantitative study. Exp. Brain Res. 70, 569–576.

Mima, T., Ikeda, A., Terada, K., Yazawa, S., Mikuni, N., Kunieda, T., Taki, W., Kimura, J., Shibasaki, H., 1997. Modality-specific organization for cutaneous and proprioceptive sense in human primary sensory cortex studied by chronic epicortical recording. Electroencephalogr. Clin. Neurophysiol. 104, 103-107.

Mima, T., Hallett, M., 1999. Corticomuscular coherence: a review. J. Clin. Neurophysiol. 16, 501–511.

Mima, T., Steger, J., Schulman, A.E., Gerloff, C., Hallett, M., 2000. Electroencephalographic measurement of motor cortex control of muscle activity in humans. Clin. Neurophysiol. 111, 326–337.

Mima, T., Matsuoka, T., Hallett, M., 2001. Information flow from the sensorimotor cortex to muscle in humans. Clin. Neurophysiol. 112, 122–126.

Murayama, N., Lin, Y.Y., Salenius, S., Hari, R., 2001. Oscillatory interaction between human motor cortex and trunk muscles during isometric contraction. Neuroimage 14, 1206–1213.

Nakahara, H., Nakasato, N., Kanno, A., Murayama, S., Hatanaka, K., Itoh, H., Yoshimoto, T., 2004. Somatosensory-evoked fields for gingiva, lip, and tongue. J. Dent. Res. 83, 307–311.

Onishi, H., Oyama, M., Soma, T., Kirimoto, H., Sugawara, K., Murakami, H., Kameyama, S., 2011. Muscle-afferent projection to the sensorimotor cortex after voluntary movement and motor-point stimulation: an MEG study. Clin. Neurophysiol. 122, 605–610.

Piitulainen, H., Bourguignon, M., De Tiège, X., Hari, R., Jousmäki, V., 2013a. Corticokinematic coherence during active and passive finger movements. Neuroscience 238, 361–370.

Piitulainen, H., Bourguignon, M., De Tiège, X., Hari, R., Jousmäki, V., 2013b. Coherence between magnetoencephalography and hand-action-related acceleration, force, pressure, and electromyogram. Neuroimage 72, 83–90.

Riddle, C.N., Baker, S.N., 2005. Manipulation of peripheral neural feedback loops alters human corticomuscular coherence. J. Physiol. 566, 625–639.

Riddle, C.N., Baker, S.N., 2006. Digit displacement, not object compliance, underlies task dependent modulations in human corticomuscular coherence. Neuroimage 33, 618–627.

Rosenberg, J.R., Amjad, A.M., Breeze, P., Brillinger, D.R., Halliday, D.M., 1989. The Fourier approach to the identification of functional coupling between neuronal spike trains. Prog. Biophys. Mol. Biol. 53, 1–31.

Ruspantini, I., Saarinen, T., Belardinelli, P., Jalava, A., Parviainen, T., Kujala, J., Salmelin, R., 2012. Corticomuscular coherence is tuned to the spontaneous rhythmicity of speech at 2-3 Hz. J. Neurosci. 32, 3786–3790.

Salenius, S., Salmelin, R., Neuper, C., Pfurtscheller, G., Hari, R., 1996. Human cortical 40 Hz rhythm is closely related to EMG rhythmicity. Neurosci. Lett. 213, 75–78.

Salenius, S., Portin, K., Kajola, M., Salmelin, R., Hari, R., 1997. Cortical control of human motoneuron firing during isometric contraction. J. Neurophysiol. 77, 3401–3405.

Sakamoto, K., Nakata, H., Kakigi, R., 2008. Somatosensory-evoked magnetic fields following stimulation of the tongue in humans. Clin. Neurophysiol. 119, 1664–1673.

Sarvas, J., 1987. Basic mathematical and electromagnetic concepts of the biomagnetic inverse problem. Phys. Med. Biol. 32, 11–22.

Schwarz, D.W., Deecke, L., Fredrickson, J.M., 1973. Cortical projection of group I muscle afferents to areas 2, 3a, and the vestibular field in the rhesus monkey. Exp. Brain. Res. 17, 516–526.

Schelter, B., Winterhalder, M., Eichler, M., Peifer, M., Hellwig, B., Guschlbauer, B., Lücking, C.H., Dahlhaus, R., Timmer, J., 2006. Testing for directed influences among neural signals using partial directed coherence. J. Neurosci. Methods 152, 210–219.

Stål, P., Marklund, S., Thornell, L.E., De Paul, R., Eriksson, PO., 2003. Fibre composition of human intrinsic tongue muscles. Cells. Tissues. Organs. 173, 147–161.

Wessberg, J., Vallbo, A.B., 1995. Coding of pulsatile motor output by human muscle afferents during slow finger movements. J. Physiol. 485, 271–282.

Welch, P., 1967. The use of fast Fourier transform for the estimation of power spectrum: a method based on time averaging over short, modified periodograms. IEEE Trans. Audio Electroacous. 15, 70–73.

Witham, C.L., Riddle, C.N., Baker, M.R., Baker, S.N., 2011. Contributions of descending and ascending pathways to corticomuscular coherence in humans. J. Physiol. 589, 3789–3800.

van Wijk, B.C., Beek, P.J., Daffertshofer, A., 2012. Neural synchrony within the motor system: what have we learned so far? Front. Hum. Neurosci. 6, 252.

Xiang, J., Hoshiyama, M., Koyama, S., Kaneoke, Y., Suzuki, H., Watanabe, S., Naka, D., Kakigi, R., 1997. Somatosensory evoked magnetic fields following passive finger movement. Brain Res. Cogn. Brain Res. 6, 73–82.

Table 1.

Peak frequencies of muscular-muscular coherence between tongue sides and the cortico-muscular coherence at the low-frequency band.

	MMC (Hz)		CMC (Hz)							
			Right				Left			
			Contra.		Ipsi.		Contra.		Ipsi.	
Sub.	F	S	F	S	F	S	F	S	F	S
1	3	9	3	7	2	7	3	7	2	10
2	N	9	N	7	3	8	3	8	2	8
3	3	10	5	8	5	8	4	10	4	10
4	3	7	4	N	N	7	N	7	N	9
5	3	6	3	6	4	9	5	8	3	6
6	3	6	3	8	3	7	2	7	2	7
7	3	6	3	6	2	6	3	N	3	N
8	3	6	4	8	2	10	2	6	4	8
9	3	7	N	N	N	N	N	N	N	N
10	3	7	4	6	2	6	2	6	4	6
11	2	7	3	7	4	8	2	8	4	7
12	3	7	2	7	2	8	2	8	2	7
13	4	10	2	8	2	7	3	7	2	8
14	3	6	3	N	4	9	3	7	5	7
15	N	9	3	10	2	10	4	10	4	10
16	N	6	2	7	4	10	2	8	3	8

17	2	8	4	10	4	N	3	6	4	N
18	2	7	2	7	3	9	4	8	2	7
19	2	7	3	8	4	7	3	7	3	7
20	3	8	2	7	2	7	2	7	2	7
21	3	8	2	6	2	7	2	7	3	6
Range	2–4	6–10	2–5	6–10	2–5	6–10	2–5	6–10	2–5	6–10
Mean ±	2.8	7.4	3.0	7.4	2.9	7.9	2.8	7.5	3.1	7.7
SEM	±	±	±	±	±	±	±	±	±	±
	0.1	0.3	0.2	0.3	0.2	0.3	0.2	0.3	0.2	0.3

MMC, Muscular-muscular coherence between tongue sides; CMC, Cortico-muscular coherence; Contra., Contralateral hemisphere; Ipsi., Ipsilateral hemisphere; Sub., Subject number; F, First peak; S, Second peak; N, Not detected; SEM, Standard error of the mean.

Table 2.

Mean values of the cortico-muscular coherence at the low-frequency band and β band.

	Low-CMC								β-CMC			
	Right				Left				Right		Left	
	Contra.		Ipsi.		Contra.		Ipsi.		Contra.	Ipsi.	Contra.	Ipsi.
	F	S	F	S	F	S	F	S				
Mean	0.0178	0.0192	0.0159	0.0175	0.0188	0.0189	0.0186	0.0167	0.0182	0.0145	0.0194	0.0146
SEM	0.0021	0.0030	0.0014	0.0015	0.0040	0.0021	0.0031	0.0023	0.0014	0.0014	0.0015	0.0007

Low-CMC, Cortico-muscular coherence at the low-frequency band; β-CMC, Cortico-muscular coherence at the β band; Contra., Contralateral hemisphere; Ipsi., Ipsilateral hemisphere; F, First peak; S, Second peak; SEM, Standard error of the mean.

Figure legends

Figure 1. Example electromyographic (EMG) signals recorded from subject 10. EMG recorded from both sides of the tongue muscles during tongue protrusion. Note that the cyclical EMG activity (indicated by arrows) was synchronized at the low-frequency band between the sides of the tongue. Rt. EMG, EMG signal recorded from the right side of the tongue; Lt. EMG, EMG signal recorded from the left side of the tongue.

Figure 2. Single subject (subject 10) data during the tongue protrusion task. **A.** Power spectra for the magnetoencephalography (MEG) signal **[1]** recorded from a sensor over the right hemisphere, and for the electromyography (EMG) signal **[2]** recorded from the left tongue muscles. Both spectra are plotted on a logarithmic scale. Each trace runs from 0 to 35 Hz. Distinct peaks in these spectra were detected at 10 and 19 Hz for the MEG signal and at 3, 7, and 24 Hz for the EMG. **B.** Muscular-muscular coherence (MMC) spectrum between sides of the tongue shows clear peaks at 3, 7, and 24 Hz. The spectra of EMG power and MMC have two distinct peaks at 3 and 7 Hz in the low-frequency band of 2–10 Hz. **C.** Cortico-muscular coherence (CMC) spectra for the left [1] and right [2] sides of the tongue. Each trace goes from 0 to 35 Hz. The horizontal gray line in each column indicates the 99% significance level. For the left side of the tongue, coherent signals were observed at 2, 6, and 26 Hz over the contralateral hemisphere and at 4, 6, and 23 Hz over the ipsilateral hemisphere. For the right side of the tongue, coherent signals were detected at 4, 6, and 25 Hz over the contralateral hemisphere and at 2, 6, and 24 Hz over the ipsilateral hemisphere. The CMC peak frequency has two distinct peaks over both hemispheres for each side of the

tongue in the low-frequency band of 2–10 Hz. Contra., Contralateral hemisphere; Ipsi., Ipsilateral hemisphere.

Figure 3. A. Cross-correlogram and somatosensory evoked field (SEF) waveforms over the contralateral sensors for the right side of the tongue in subject 10. **[1]** Cross-correlogram of cortico-muscular coherence (CMC) at 2–10 Hz (low-CMC). The trace starts 500 ms before and ends 500 ms after electromyography (EMG) onset. The vertical line indicates the time of zero lag. The largest magnetoencephalography (MEG) signal peak occurred at 69 ms after EMG onset. **[2]** Cross-correlogram of CMC at 15–35 Hz (β-CMC). The trace starts 100 ms before and ends 100 ms after EMG onset. The largest MEG signal peak occurred 8 ms before EMG onset. **[3]** SEFs by electrical tongue stimulation. The trace starts 50 ms before and ends 500 ms after stimulation onset. The largest peak was detected at 71 ms after stimulus onset. **B**. Isocontour maps over the contralateral (left) hemisphere for the CMC and SEFs in subject 10. The contour map was obtained from the time points showing waveform peaks in the cross-correlograms and SEFs. Red and blue lines indicate outgoing and incoming magnetic fluxes, respectively. Green arrows show the location and direction of equivalent current dipoles (ECDs) projected on the skull surface. Arrowheads indicate the negative pole of the ECDs. The isofield contour maps showed a dipolar pattern at the latency showing the maximum amplitude. The directions of ECDs were posterior for the low-CMC and SEFs, but anterior for the β-CMC. **C**. ECD locations over the left hemisphere for the CMC and SEFs in subject 10. The ECDs of the low-CMC and SEFs were located in the lateral part of the central sulcus. The ECDs of the β-CMC were located in the anterior part of the central sulcus.

Figure 4. Conduction time from the tongue to the cortex for the cortico-muscular coherence (CMC) and somatosensory evoked fields (SEFs) across subjects (mean ± the standard error of the mean). Cortical activation followed muscle activation for the CMC at 2–10 Hz (low-CMC) and cortical activation followed electrical stimulation for SEFs. However, the cortical responses preceded muscle activity for the CMC at 15–35 Hz (β-CMC). The mean conduction times were not significantly different between the low-CMC and SEFs. NS, Not significant.

Figure 5. Averaged dipole locations on the *x*-, *y*-, and *z*-axes for the cortico-muscular coherence (CMC) and somatosensory evoked fields (SEFs) across subjects. Data points represent the mean ± the standard error of the mean. The locations of the equivalent current dipoles (ECDs) for the CMC at 2–10 Hz (low-CMC) were significantly posterior, but not inferior or left to those for the CMC at 15–35 Hz (β-CMC). Moreover, the ECD locations for the low-CMC were not significantly different to those of the SEFs in each axis. The ECD locations for the SEFs were located significantly posterior, inferior, and left to those for the β-CMC. The *x*-axis passes through the preauricular points from left to right, while the *y*-axis passes through the nasion, and the *z*-axis points upward from the plane determined by the *x*- and *y*-axes. NS, Not significant.

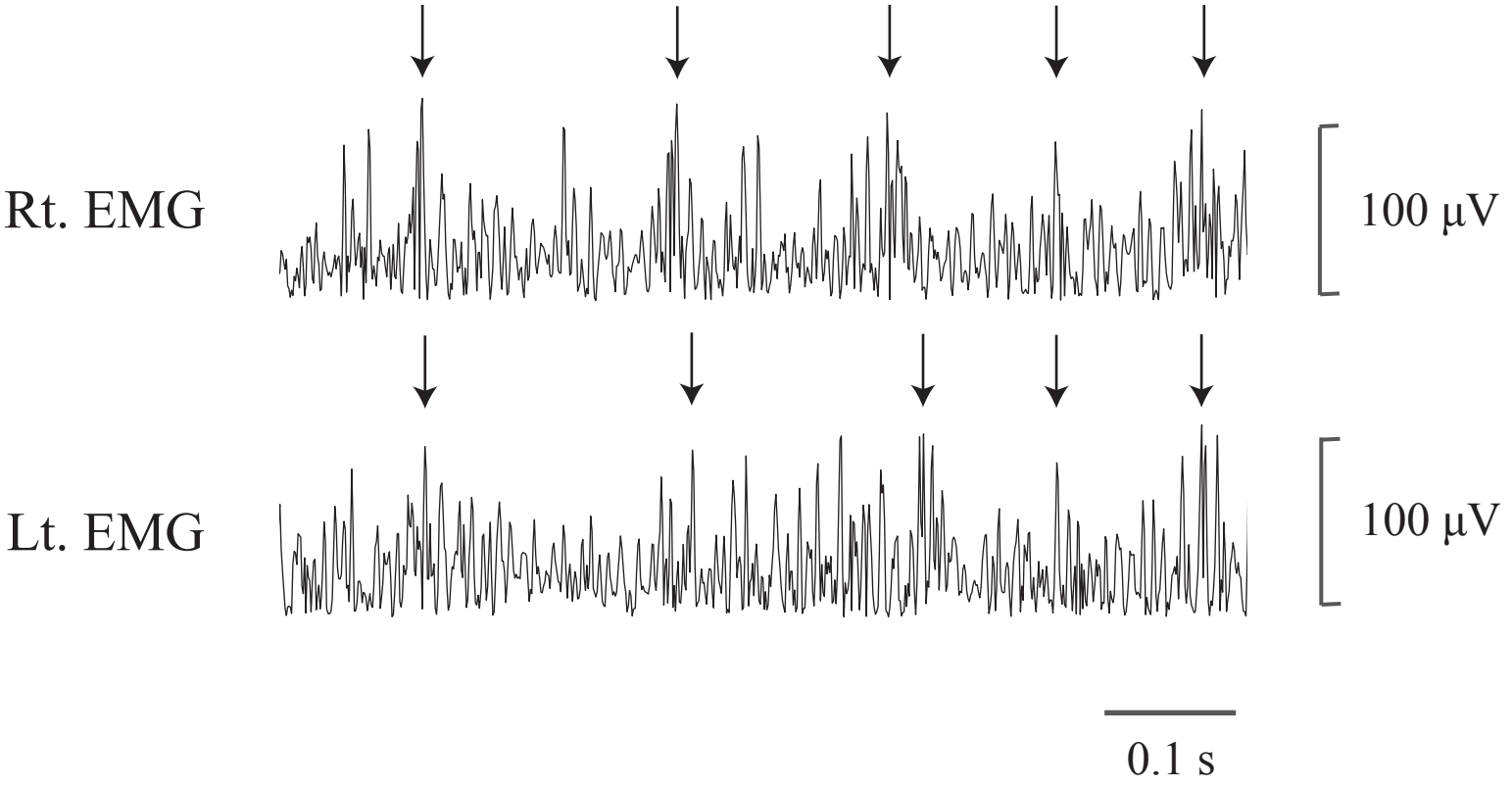
Rt. EMG
100 μV
Lt. EMG
100 μV
0.1 s

A. Power spectra

[1] MEG

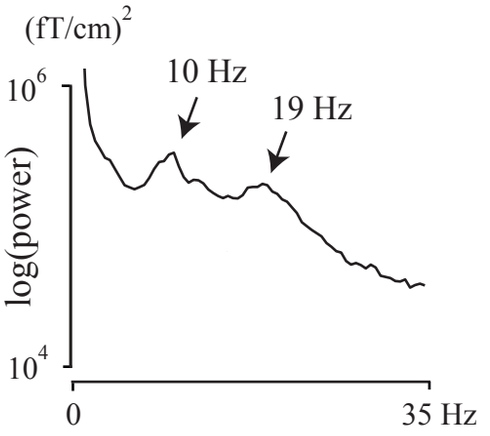

[2] EMG

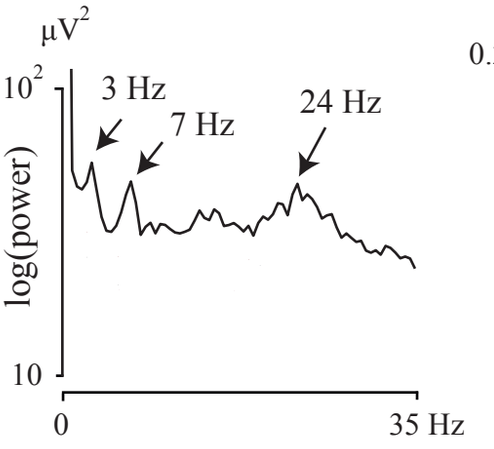

B. Muscular-muscular coherence between sides

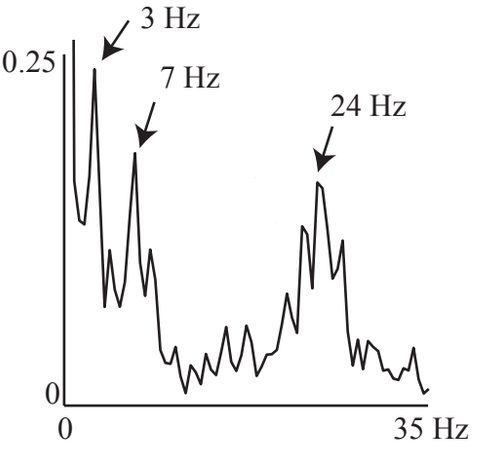

C. Cortico-muscular coherence

[1] Left side of the tongue

Contra.

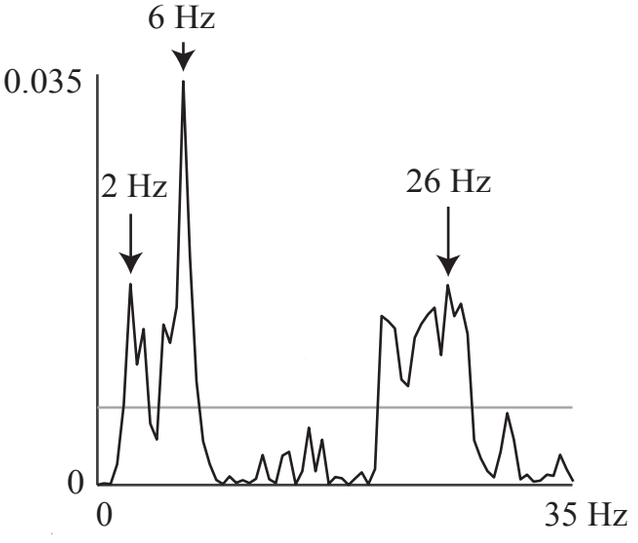

Ipsi.

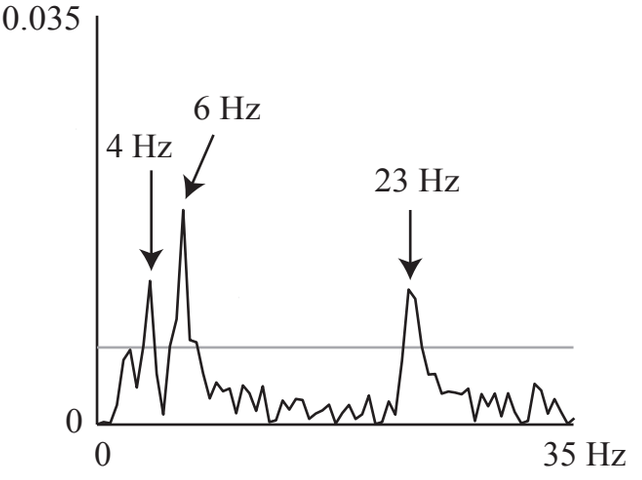

[2] Right side of the tongue

Contra.

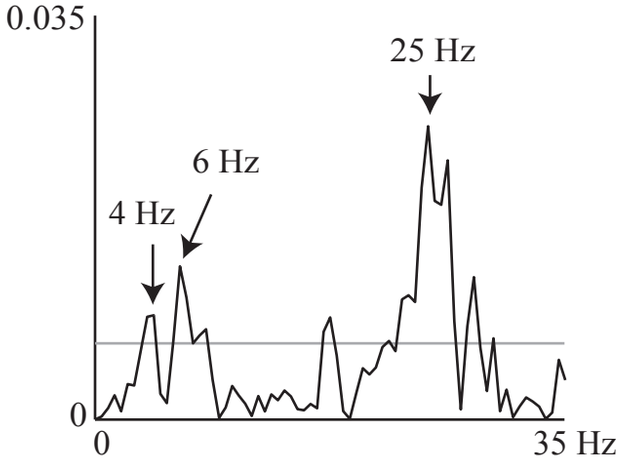

Ipsi.

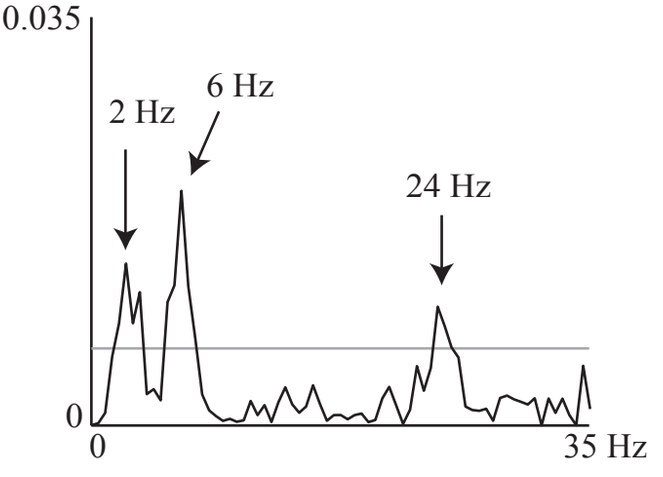

A. Cross-correlograms and SEF waveforms

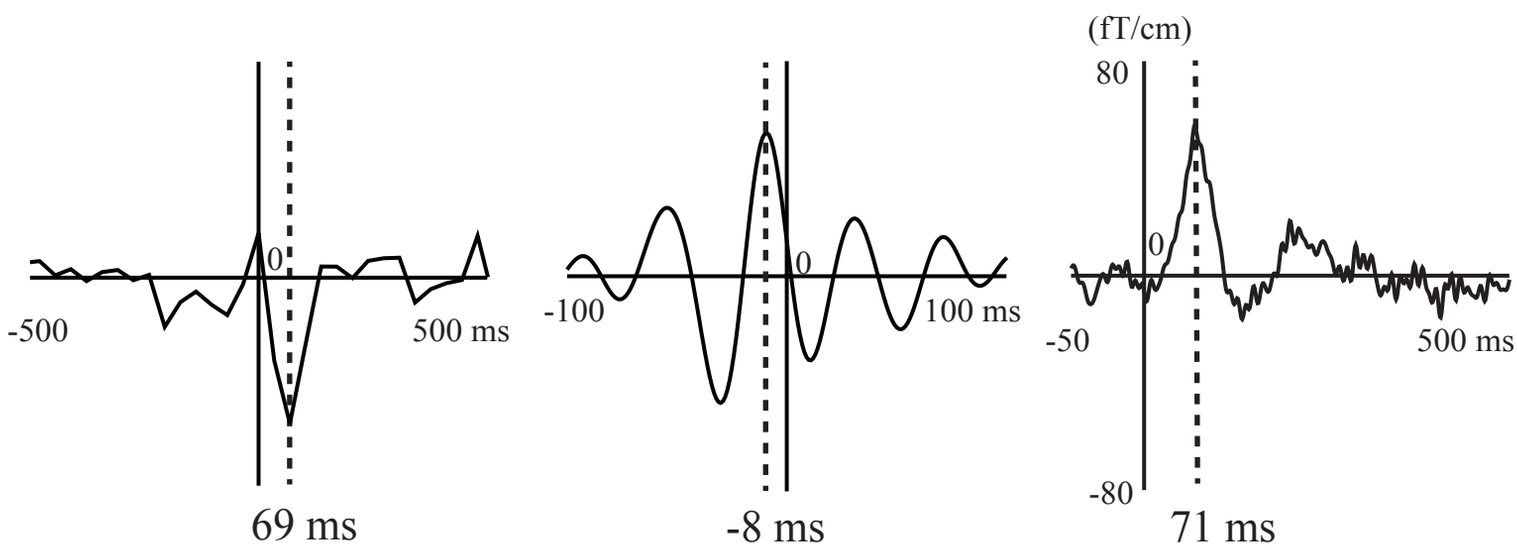

B. Isocontour maps

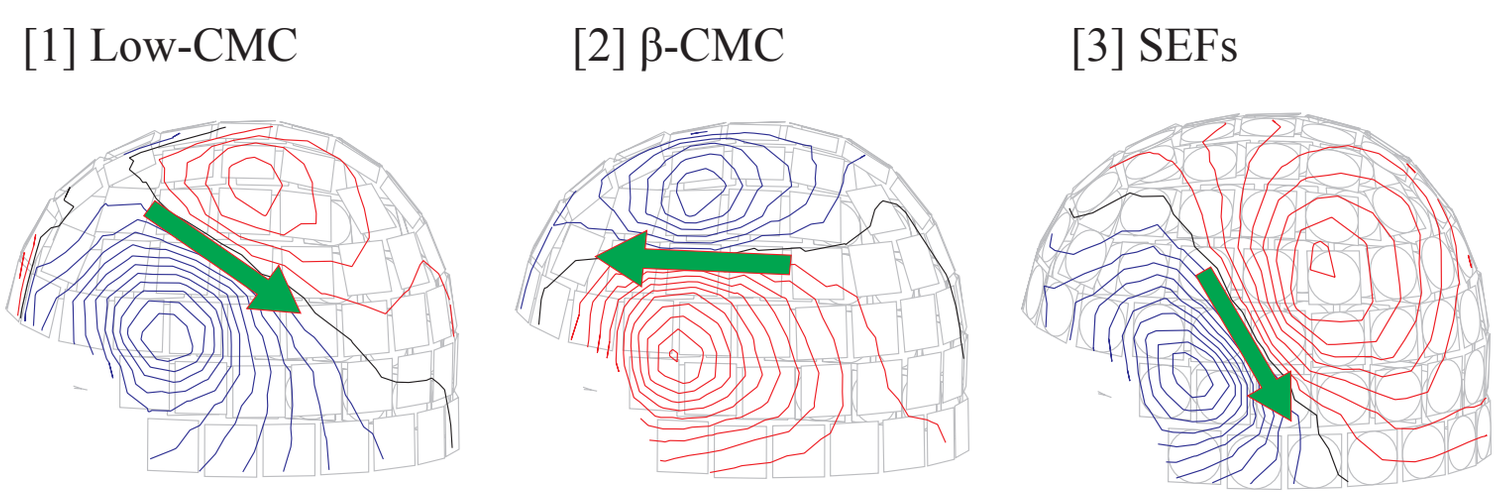

C. Dipole locations and orientations of the CMC and SEFs

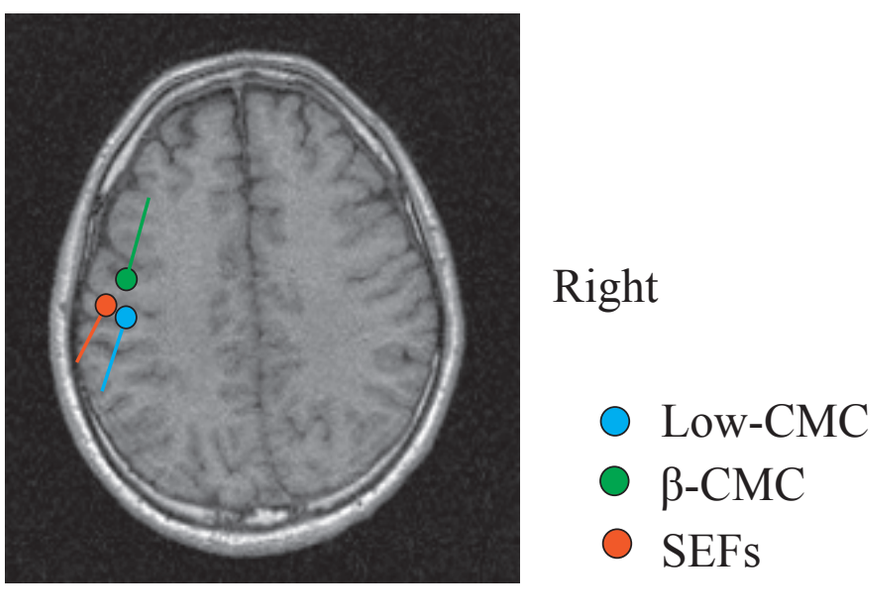

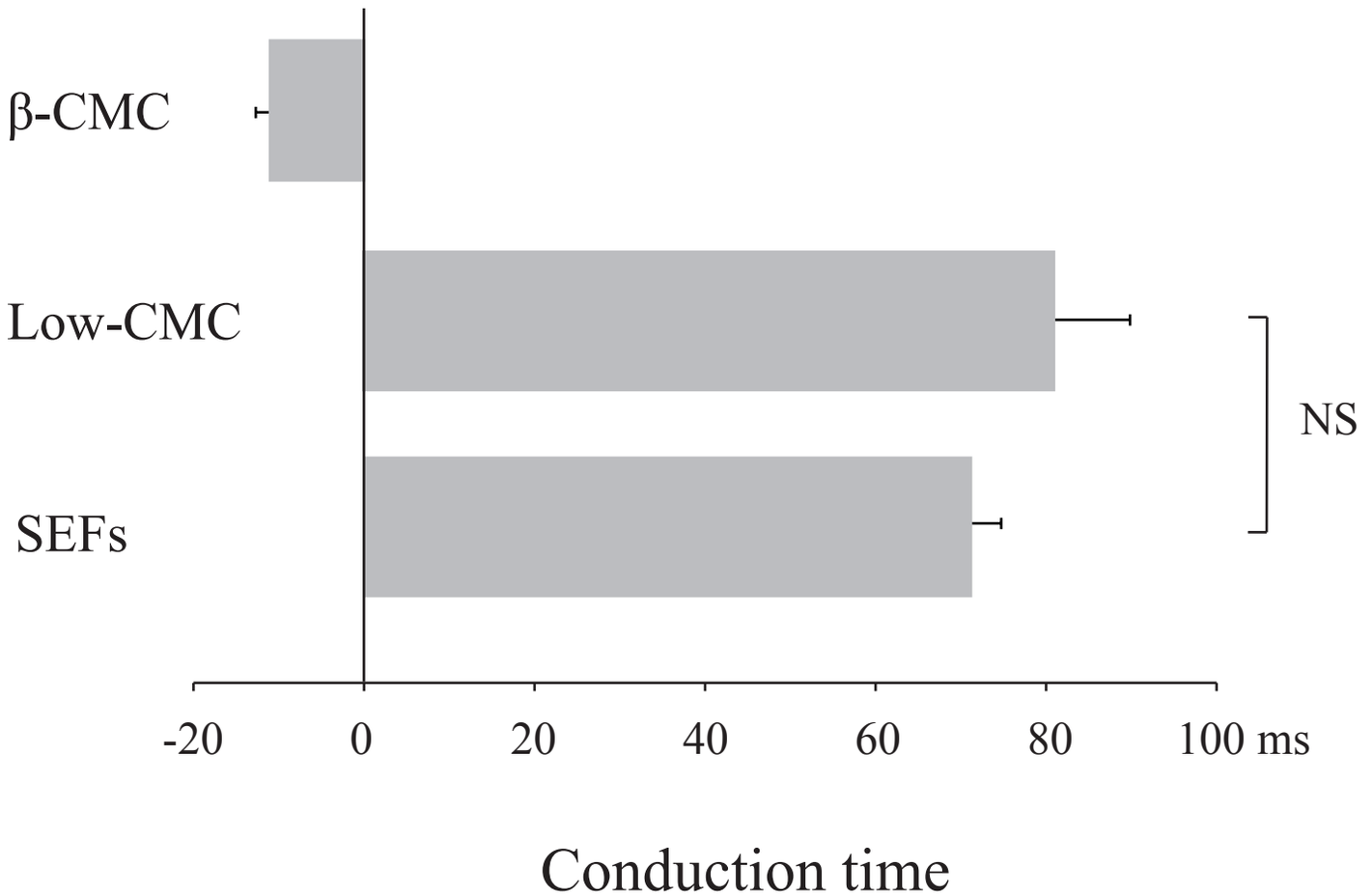
β-CMC
Low-CMC
SEFs
NS
-20
0
20
40
60
80
100 ms
Conduction time

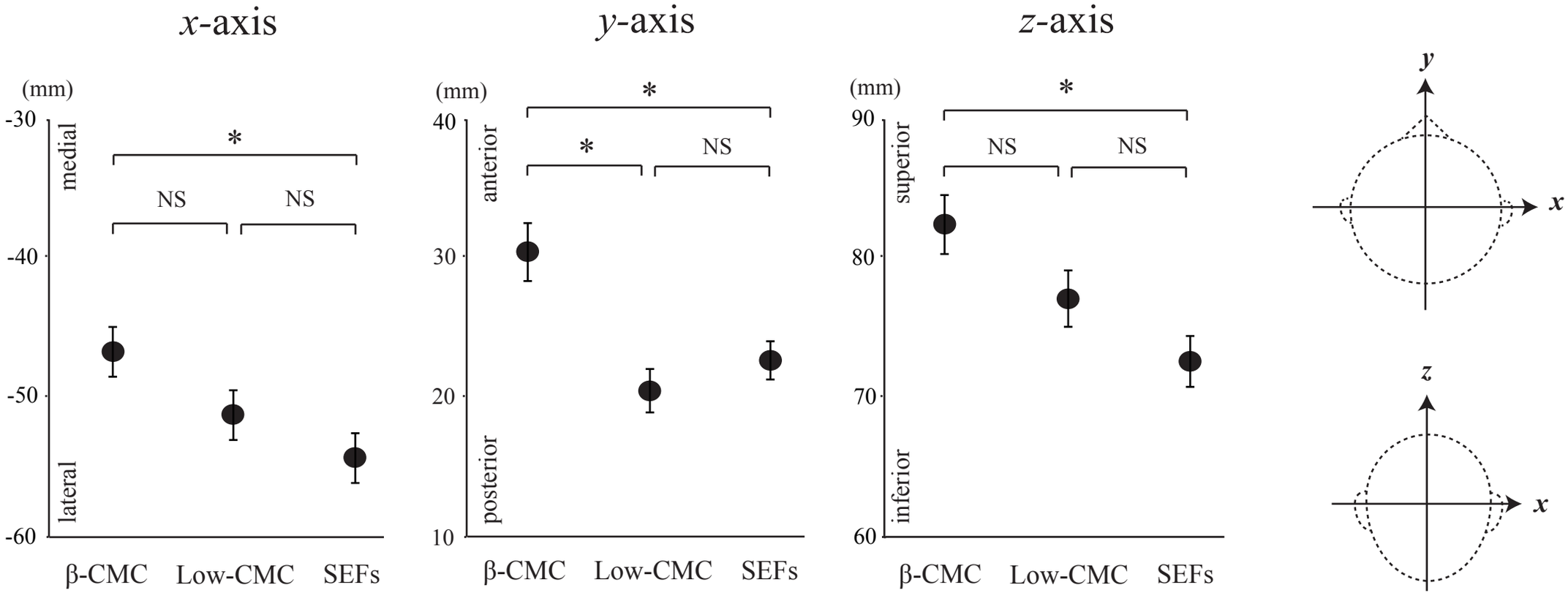
x-axis
(mm)
-30
-40
-50
-60
medial
lateral
*
NS
NS
β-CMC
Low-CMC
SEFs
y-axis
(mm)
40
30
20
10
anterior
posterior
*
*
NS
β-CMC
Low-CMC
SEFs
z-axis
(mm)
90
80
70
60
superior
inferior
*
NS
NS
β-CMC
Low-CMC
SEFs
y
x
z
x